

Thin-Film Physics Group (Application-oriented thin-film research)

0.1 Epitaxial IV-VI narrow-gap semiconductor layers

M. Arnold, F. Felder, M. Rahim, A.N. Tiwari, and H. Zogg; www.tfp.ethz.ch

Narrow gap lead chalcogenide (IV-VI) layers like PbX , $\text{Pb}_{1-x}\text{Sn}_x\text{X}$, $\text{Pb}_{1-y}\text{Eu}_y\text{X}$ and $\text{Pb}_{1-y}\text{Sr}_y\text{X}$ ($\text{X}=\text{Te}$, Se) are investigated for applications and basic research. The band gaps of the active infrared layers are between 0.1 and 0.25 eV (corresponding to wavelengths in the mid-IR range). Larger band gaps are realised with larger y values for the cladding $\text{Pb}_{1-y}\text{Eu}_y\text{X}$ and $\text{Pb}_{1-y}\text{Sr}_y\text{X}$ layers. All layers are grown by solid source molecular beam epitaxy (MBE) onto Si(111)-substrates by employing a CaF_2 buffer layer, or onto $\text{BaF}_2(111)$ substrates. The layers are heavily lattice- and (for Si-substrates) thermal-expansion mismatched. Misfit and threading dislocations therefore are present. However, lead-chalcogenides are fault tolerant. Even with threading dislocations densities in the 10^7 cm^{-2} to 10^8 cm^{-2} range, optoelectronic devices with reasonable quality are obtained. The minority carrier lifetimes τ are determined by the density of the threading dislocations ρ , $\tau \sim 1/\rho$.

We have realized photovoltaic infrared detectors and applied them to fabricate complete heteroepitaxial monolithic two-dimensional Infrared Focal Plane Arrays (2d IR-FPA) on active Si-substrates. As IR-sources, we fabricated optically pumped edge-emitting mid-IR lasers, again on Si-substrates.

In addition, it is easy to fabricate Bragg mirrors with very high reflectivity over a broad spectral range. These mirrors consist of quarter wavelength stacks of layers with alternating high (n_H) and low (n_L) refractive indices. With the materials typically used, EuSe ($n_L=2.4$) or BaF_2 ($n_L=1.4$) with low indices, PbX or $\text{Pb}_{1-x}\text{Sn}_x\text{X}$ ($n_H>4$) with high indices, two to three quarter wavelength n_L/n_H pairs suffice to obtain reflection coefficients $>99\%$. With such mirrors, complete Fabry-Perot cavities can be grown.

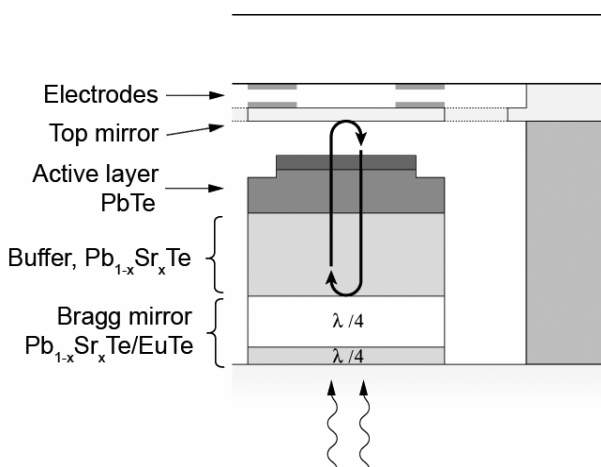


Fig. 1: Design of a tuneable mid-infrared RCED with a moveable electro statically actuated top mirror.

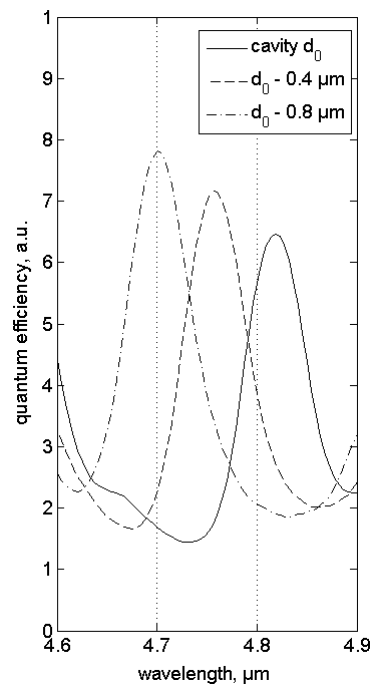


Fig. 2: Measured sensitivity spectrum of a tuneable RCED at three different distances, d_0 , $d_0 - 0.4 \mu\text{m}$ and $d_0 - 0.8 \mu\text{m}$, of the top mirror (95 K).

By placing the active detector layer inside the cavity, a **resonant cavity enhanced detector (RCED)** is obtained. It is sensitive at the resonance wavelengths only where it exhibits a high quantum efficiency. The positions of the resonances are determined by the length of the cavity. With a monolithic approach, this length is determined by the optical path inside the cavity and is fixed. To obtain a tunable cavity length, the top mirror is arranged on a free standing membrane whose distance with respect to the second bottom mirror can be varied by e.g. micromechanical means (*Fig. 1*). Such an arrangement forms a micro infrared spectrometer. *Fig. 3* shows calculated results of the wavelength dependent peak quantum efficiency as a function of the position of the top mirror. A first design was realised to demonstrate the principle. A preliminary spectral response for two different cavity lengths is shown in *Fig. 2*.

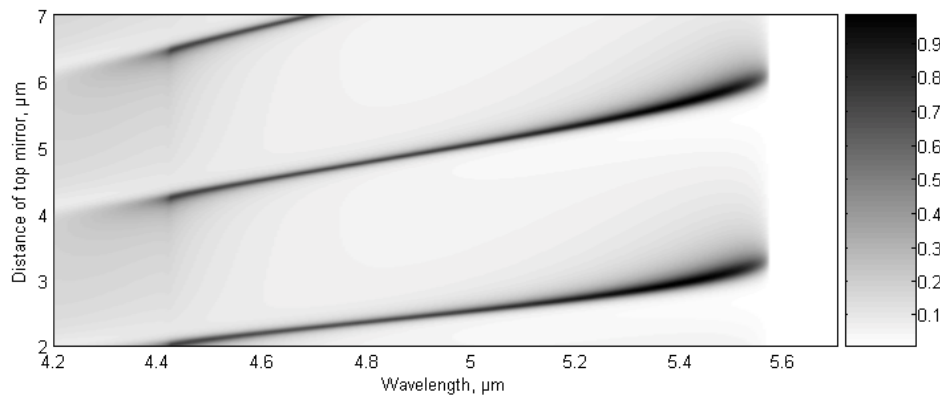


Fig. 3: Simulated quantum efficiency of a tunable PbTe RCED as a function of wavelength and mirror distance.

Another application of a Fabry-Perot cavity with a tunable top mirror is the **vertical external cavity surface emitting laser (VECSEL)**. Monolithic vertical cavity surface emitting lasers (VCSELs) have become technologically important up to the near-IR range because of their easy planar processing, and their small beam divergence which results in a good beam quality. A VECSEL is defined as half VCSEL with an external curved mirror. The cavity length is tunable by moving the external mirror, which allows the tuning of the output wavelength over quite a broad range.

We realized the first VECSEL for the mid-IR range by using IV-VI narrow bandgap materials. As already stated, high reflection Bragg mirrors are easily obtained with IV-VI compounds. The active layer of the VECSEL simply consists of a a few μm thick PbTe layer. It is pumped optically with a commercial laser diode with $1.55 \mu\text{m}$ wavelength (**Fig. 4**). The maximum emission wavelength at 150K operation temperature is $4.96 \mu\text{m}$ with a pump power slightly above threshold. Here, the spectrum is nearly monomode (**Fig. 5**, right curve). The wavelength shifts to shorter values at higher pump-powers due to heating of the active layer (**Fig. 5**, right curve).

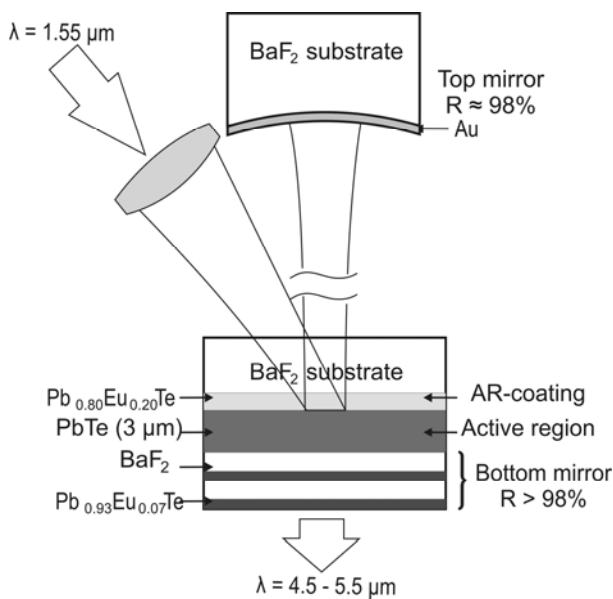


Fig. 4: Schematic representation of the VECSEL.

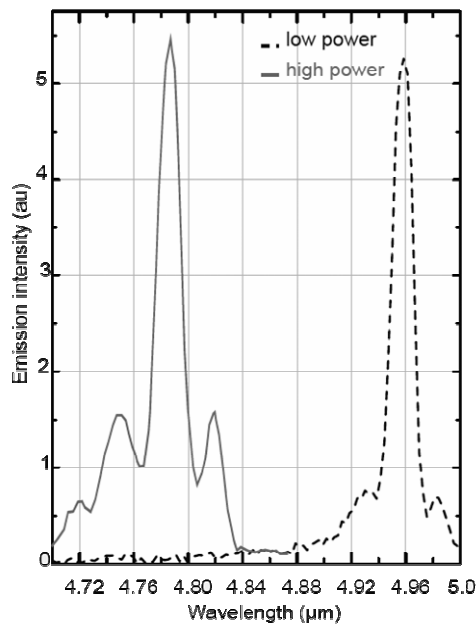


Fig. 5: Spectra of VECSEL at 150 K. Right curve: One dominating mode at low pumping power; left curve: Multimode emission at higher pumping power

0.2 Thin-film solar cells based on Cu(In,Ga)Se₂ compound semiconductors

D. Brémaud, S. Bücheler, A. Chirila, K. Ernits, R. Verma, M. Kaelin, H. Zogg, and A.N.Tiwari; www.tfp.ethz.ch

Safe, cheap, abundant, renewable, and environment-friendly generation of electricity is of considerable interest for our society. Thin-film solar cell technology based on the polycrystalline compound semiconductor Cu(In,Ga)Se₂ (usually abbreviated as "CIGS") is a very promising solution for this task. New cell concepts to improve the stability and efficiency are among further projects.

Alternative Transparent Back Contacts

Tandem solar cells (two or more stacked solar cells) are important to further improve the photovoltaic conversion efficiency by better utilization of the solar spectrum. CIGS for such applications require transparent electrical back contacts. Therefore, the conventional Mo contact for CIGS has to be replaced with an appropriate transparent conducting layer. We have developed CIGS solar cells with a transparent conductive oxide, ITO, as back contact. To facilitate or allow the formation of an ohmic contact a very thin MoSe₂ interface layer has been applied between ITO and CIGS to obtain carrier transport through tunneling. Therefore, Mo layers have been sputtered on the ITO and selenized before the deposition of CIGS. The MoSe₂ layers have been investigated to determine the thickness of MoSe₂ and the converted ratio of Mo. CIGS layers were then grown by evaporation of elemental Cu, In, Ga, and Se, at a max. temperature of 450°C. Because the used alternative back contacts act as barrier and inhibit the Na diffusion from the glass substrate, we have added Na separately using a post deposition treatment. The properties of CIGS layers with and without Na have been investigated by different methods (SEM, SIMS, EDX). The photovoltaic properties of small area solar cells were characterized with I-V and quantum efficiency

measurements. Under simulated AM1.5 standard test conditions an efficiency of 11.9% ($V_{oc} = 603$ mV, $J_{sc} = 31.4$ mA.cm⁻², FF= 63.1 %, total area = 0.6 cm², no ARC) with ITO back contacts has been achieved on SLG substrates.

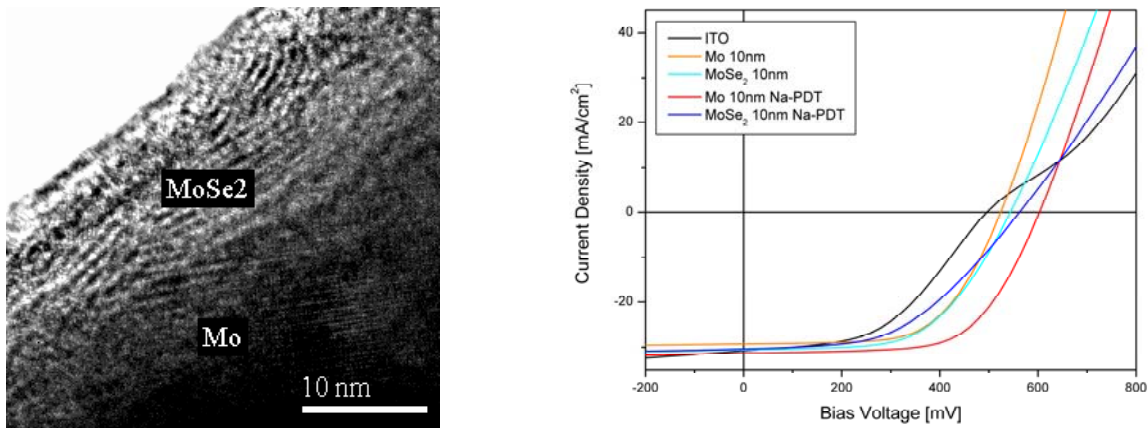


Figure 6: *Left:* High resolution transmission electron microscope (HRTEM) image of thin Mo-layer showing formation of MoSe₂. *Right:* J-V measurements showing the improving effect of MoSe₂-layer and Na post deposition treatment (Na-PDT)

Ultrasonic sprayed In_xS_y

In₂S₃ films produced by ultrasonic spray pyrolysis (USP) method are developed as an alternative buffer-layer for CIGS solar cells. We have optimized the In₂S₃ spray process parameters and investigated the properties of USP-In₂S₃ layers grown at different substrate temperatures and spray solution concentrations. Thickness measurements showed that the film growth rate increases with substrate temperature and precursor concentration in the solution. Optical transmission decreased with higher substrate temperature and lower thiourea concentration in the spray solution. Scanning Electron Microscopy (SEM) images showed that continuous thin In₂S₃ buffer-layers have been grown on glass substrates. X-ray Diffraction (XRD) and X-ray Photoelectron Spectroscopy (XPS) measurements revealed that mainly In₂S₃ phases were formed in the films. We achieved solar cell efficiencies up to 9.5 % for CIGS/In₂S₃ cells after light soaking, compared to 12.9 % efficiency for CIGS cell with a standard chemical bath deposited CdS buffer-layer.

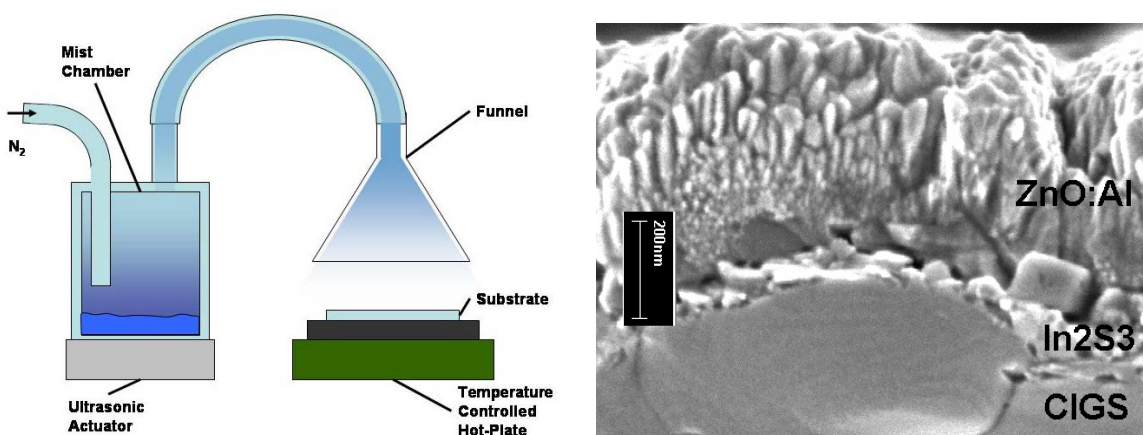


Figure 7: *Left:* Schematic of the USP system; mist of the solution generated by the ultrasonic actuator is transported through a tube and the funnel for a spray. *Right:* SEM cross-section image of the CIGS solar cell with USP-In₂S₃ as a buffer-layer.

Upscaling of flexible CIGS solar cells

Flexible solar cells on polyimide foil of $5 \times 5 \text{ cm}^2$ have been developed using vacuum evaporated CIGS layer and we have achieved conversion efficiencies up to 14.1%, which is a record for any kind of solar cell grown on polymer foil. We have started the upscaling of the deposition process to grow layers on $30 \times 30 \text{ cm}^2$ size substrates by in-house assembly of a CIGS deposition system. Development of large area flexible solar cells and mini-modules has started, and as a proof of concept flexible mini-modules to run small ventilator-fans have been made. A mini-module with a 16 cm^2 total area efficiency of 7.9% has been developed. The factors for further efficiency improvements were identified although this result is already among the most efficient solar modules produced on polymer foil.

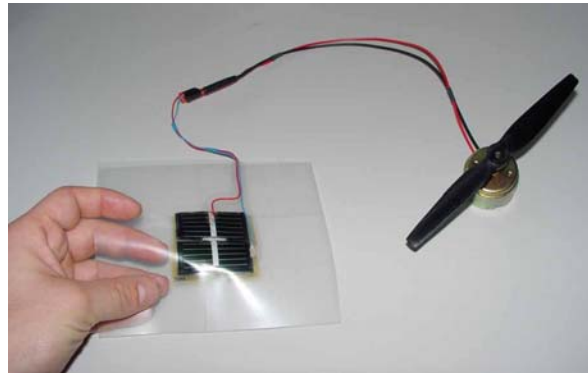
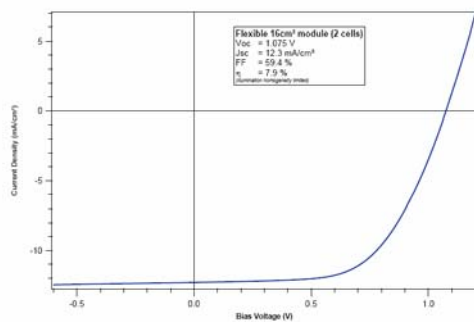


Figure 8: *Left:* J-V curve of 16 cm^2 mini-module obtained by connection of two large area cells with metal grids. *Right:* Flexible mini-module to run a ventilator-fan.